

Tetrathiafulvalene-*s*-tetrazine: versatile platform for donor-acceptor systems and multifunctional ligands

Flavia Pop, Jie Ding, Latévi Max Lawson Daku, Andreas Hauser and Narcis Avarvari*

SUPPORTING INFORMATION

Experimental section

General comments. Reactions were carried out under Argon and using toluene HPLC. Nuclear magnetic resonance spectra were recorded on a Bruker Avance DRX 500 spectrometer (operating at 500.04 MHz for ¹H and 125 MHz for ¹³C) and Bruker Avance DRX 300 automatic spectrometer (operating at 300 MHz for ¹H, and 75 MHz for ¹³C). Chemical shifts are expressed in parts per million (ppm) downfield from external TMS. The following abbreviations are used: s, singlet; d, doublet; td, triplet of doublets; ddd, doublet of doublet of doublets; m, multiplet. MALDI- TOF MS spectra were recorded on Bruker Biflex-IIITM apparatus, equipped with a 337nm N2 laser. ESI MS spectra were recorded on a Bruker Esquire 3000 plus apparatus. Elemental analyses were recorded using Flash 2000 Fisher Scientific Thermo Electron analyzer. Melting points were measured with a Stuart Scientific melting point apparatus SMP3.

3,6-Dichloro-1,2,4,5-tetrazine was synthesized in several steps as previously described. [1]

[1] (a) D. E. Chavez and M. A. Hiskey, *J. Heterocycl. Chem.* 1998, **35**, 1329; (b) M. D. Coburn, G. A. Buntain, B. W. Harris, M. A. Hiskey, K. Y. Lee and D. G. Ott, *J. Heterocycl. Chem.* 1991, **28**, 2049; (c) M. D. Helm, A. Plant and J. P. A. Harrity, *Org. Biomol. Chem.*, 2006, **4**, 4278.

TTF-chloro-1,2,4,5-tetrazine (1)

3,6-Dichloro-1,2,4,5-tetrazine (0.30 g, 2 mmol), 4-(trimethylstannylyl)-tetrathiafulvalene (0.35 g, 0.95 mmol), and Pd(PPh₃)₄ as catalyst (15% mmol) were mixed in 20 mL of dry toluene overnight at 60 °C under argon. The mixture was filtered over Celite and silica, washed with toluene followed by dichloromethane and solvents concentrated to afford the crude as a black solid. The residue was purified by column chromatography (cyclohexane/dichloromethane 1/1) to give 140 mg of black solid, yield: 46%, m. p. > 250 °C, dec.

¹H-NMR (500 MHz, CDCl₃) δ/ppm: 8.10 (s, 1H), 6.38 (d, 1H, ³J = 6.5 Hz), 6.36 (d, 1H, ³J = 6.5 Hz); ¹³C-NMR (125 MHz, CDCl₃) δ /ppm: 165.8, 159.6, 132.2, 126.5, 119.3, 118.9, 116.5, 106.3; MS (MALDI-TOF): *m/z*: 317.9 (M_{th} = 317.89); elemental analysis calcd. (%) for C₉H₃Cl₂N₃S₄: C 30.14, H 0.95, N 17.57, S 40.23; found: C 30.72, H 1.29, N 17.05, S 39.72.

Chloro-di(2-picoly)amine-1,2,4,5-tetrazine (2)

Di(2-picoly)amine (1.31 g, 6.6 mmol) in 20 ml of MTBE was added drop wise to a solution of 3,6-dichloro-1,2,4,5-tetrazine in 100 ml of MTBE. The mixture was stirred at room temperature overnight, the black solid formed was filtered, the solvent concentrated and the

crude purified by chromatography (dichloromethane/ethylacetate 1/1) to give 700 mg of red solid, yield: 67%, m. p. = 104.0 - 104.6 °C.

¹H-NMR (300 MHz, CDCl₃) δ/ppm: 8.54 (2H, m, ³J = 4.8 Hz, PyH), 7.65 (2H, td, ³J = 7.8 Hz, ⁴J = 1.8 Hz, PyH), 7.31 (2H, d, ³J = 7.8 Hz, PyH), 7.20 (2H, ddd, ³J = 4.8 Hz, ⁴J = 1.2, PyH), 5.21 (4H, s, NCH₂Py); ¹³C-NMR (75 MHz, CDCl₃) δ /ppm: 161.4, 160.2, 155.3, 148.1, 137.4, 122.9, 122.8, 52.7; ESI-MS m/z 314.00 [M+H]⁺ (M_{th} = 313.08); elemental analysis calcd. (%) for C₁₄H₁₂ClN₇: C 53.59, H 3.86, N 31.25; found: C 52.94, H 3.85, N 30.25.

TTF-di(2-picolyl)amine-1,2,4,5-tetrazine (**3**)

2 (0.47 g, 1.5 mmol), 4-(trimethylstannyl)-tetrathiafulvalene (0.66 g, 1.8 mmol) and Pd(PPh₃)₄ as catalyst (15% mmol) were refluxed in 30 mL of dry toluene overnight under argon. The residue was purified by column chromatography (cyclohexane/dichloromethane 1/1, followed by dichloromethane) to give 200 mg of black solid, yield: 28%, m. p. = 199.5 – 200.0 °C.

¹H-NMR (300 MHz, CDCl₃) δ/ppm: 8.53 (2H, m, ³J = 4.8 Hz, PyH), 7.63 (2H, td, ³J = 7.8 Hz, ⁴J = 1.8 Hz, PyH), 7.51 (1H, s, TTFH), 7.32 (2H, d, ³J = 7.8 Hz, PyH), 7.18 (2H, ddd, ³J = 4.8 Hz, ⁴J = 0.9, PyH), 6.33 (2H, s, TTFH), 5.25 (4H, s, NCH₂Py); ¹³C-NMR (125 MHz, CDCl₃) δ /ppm: 159.9, 155.9, 155.7, 149.6, 136.7, 130.1, 122.6, 122.2, 121.8, 119.2, 118.8, 113.3, 108.4, 52.6; MS (MALDI-TOF): m/z: 480.5 (M_{th} = 481.03); elemental analysis calcd. (%) for C₂₀H₁₅N₇S₄: C 49.87, H 3.14, N 20.36, S 26.63; found: C 49.24, H 3.00, N 19.91, S 27.46.

(**3**)ZnCl₂

A solution of TTF-di(2-picolyl)amine-1,2,4,5-tetrazine (**3**) (5 mg, 0.01 mmol) in 3 ml of dichloromethane was mixed with a solution of ZnCl₂ (1.4 mg, 0.01 mmol) in 3 ml of acetonitrile. Slow diffusion of diethyl ether or pentane onto this solution afforded single crystals of the desired complex **3** which was further analyzed by X-ray diffraction.

ESI-MS m/z 579.66 [M-Cl]⁺ (M_{th} = 614.89).

X-Ray structure determinations

Details about data collection and solution refinement are given in Table S1. X-ray diffraction measurements were performed on a Bruker Kappa CCD diffractometer, operating with a Mo $\text{K}\alpha$ ($\lambda=0.71073\text{ \AA}$) X-ray tube with a graphite monochromator. The structures were solved (SHELXS-97) by direct methods and refined (SHELXL-97) by full matrix least-square procedures on F². All nonhydrogen atoms were refined anisotropically. Hydrogen atoms were introduced at calculated positions (riding model), included in structure factor calculations but not refined. Crystallographic data for the two structures have been deposited with the Cambridge Crystallographic Data Centre, deposition numbers CCDC 888570 (**1**), CCDC 888571 (**3**)ZnCl₂. These data can be obtained free of charge from CCDC, 12 Union road, Cambridge CB2 1EZ, UK (e-mail: deposit@ccdc.cam.ac.uk or <http://www.ccdc.cam.ac.uk>).

Table S1. Crystal Data and Structure Refinement for **1** and (**3**)ZnCl₂

	1	(3)ZnCl ₂
formula	C ₈ H ₃ CIN ₄ S ₄	C ₂₀ H ₁₅ C ₁₂ N ₇ S ₄ Zn
M [g mol ⁻¹]	318.87	617.90
T [K]	293(2)	293(2)
crystal system	Monoclinic	Triclinic
space group	P2 ₁ /c	P-1
a [Å]	7.4751(11)	8.7852(17)
b [Å]	22.522(2)	9.2555(14)
c [Å]	7.5169(9)	16.386(4)
α [°]	90.000 (11)	74.976(17)
β [°]	109.736(9)	88.387(14)
γ [°]	90.000 (12)	72.238(14)
V[Å ³]	1191.2(3)	1223.6(4)
Z	4	2
ρ_{calcd} [g cm ⁻³]	1.778	1.677
μ [mm ⁻¹]	1.000	1.589
goodness-of-fit on F ²	1.037	1.013
final R1/wR2 [I > 2 σ (I)]	0.0516/0.0852	0.0430/0.0817
R1/wR2 (all data)	0.1116/0.1026	0.0952/0.0923

Compound 1

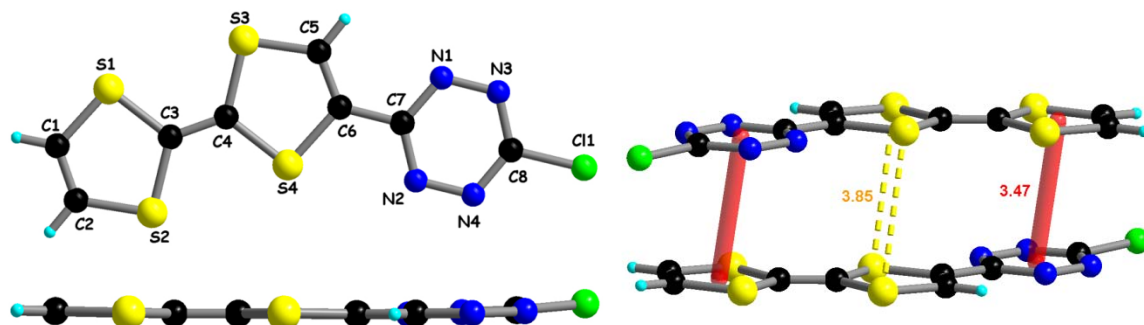


Fig. S1 Left: molecular structure of **1** with the numbering scheme (top), together with a side view of the molecule (bottom). Right: short S···S and TTF···TTZ intra-stack contacts.

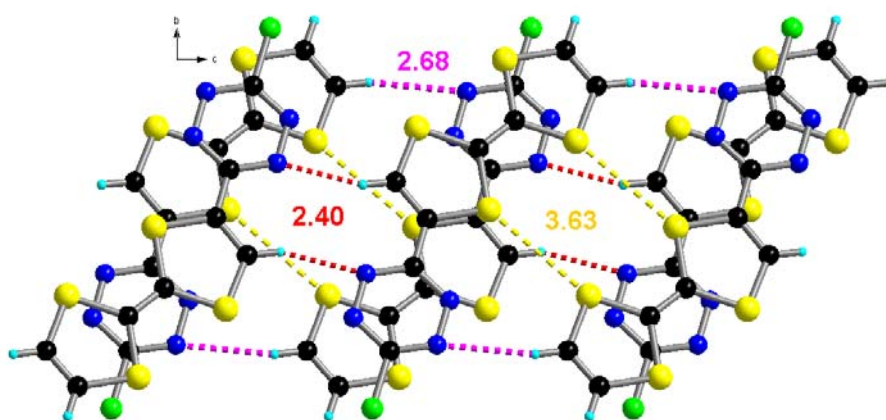


Fig. S2 Packing diagram for **1** in the *bc* plane with an emphasis on the S···S and N···H inter-stack contacts.

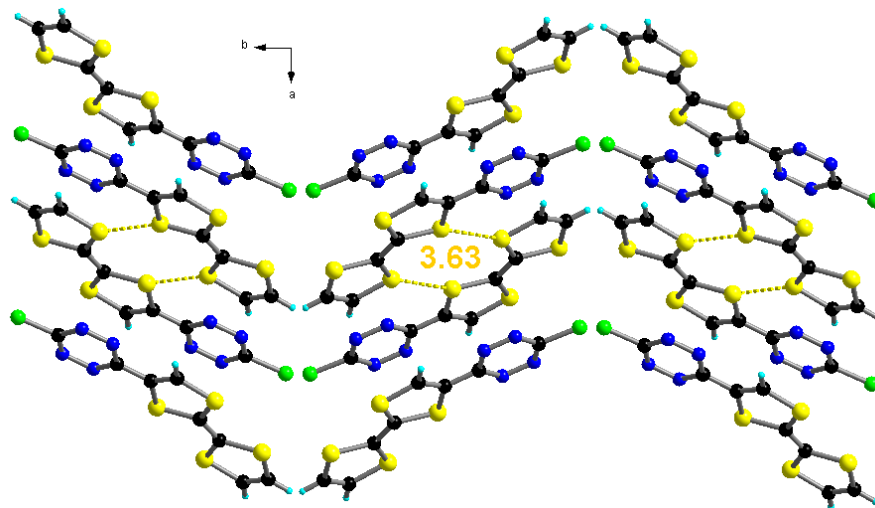


Fig. S3 Packing diagram for **1** in the *ab* plane with an emphasis on the S···S inter-stack contacts.

Table S2. Bond lengths (\AA) and angles ($^\circ$) for **1**

Bond lengths (\AA)		Bond angles ($^\circ$)	
S(1)-C(1)	1.731(4)	C(1)-S(1)-C(3)	94.54(17)
S(1)-C(3)	1.763(3)	C(2)-S(2)-C(3)	94.43(18)
S(2)-C(2)	1.737(4)	C(5)-S(3)-C(4)	94.84(15)
S(2)-C(3)	1.755(3)	C(6)-S(4)-C(4)	94.27(15)
S(3)-C(5)	1.714(3)	N(3)-N(1)-C(7)	117.2(3)
S(3)-C(4)	1.766(3)	N(4)-N(2)-C(7)	117.2(3)
S(4)-C(6)	1.753(3)	N(1)-N(3)-C(8)	116.4(3)
S(4)-C(4)	1.764(3)	C(8)-N(4)-N(2)	116.4(3)
N(1)-N(3)	1.320(4)	C(2)-C(1)-S(1)	118.3(3)
N(1)-C(7)	1.352(4)	C(2)-C(1)-H(1)	120.8
N(2)-N(4)	1.336(3)	S(1)-C(1)-H(1)	120.8
N(2)-C(7)	1.335(4)	C(1)-C(2)-S(2)	118.5(3)
N(3)-C(8)	1.338(4)	C(1)-C(2)-H(2)	120.7
N(4)-C(8)	1.323(4)	S(2)-C(2)-H(2)	120.7
Cl(1)-C(8)	1.710(3)	C(4)-C(3)-S(2)	123.3(2)
C(1)-C(2)	1.303(5)	C(4)-C(3)-S(1)	122.5(2)
C(1)-H(1)	0.9300	S(2)-C(3)-S(1)	114.18(18)
C(2)-H(2)	0.9300	C(3)-C(4)-S(4)	122.5(2)
C(3)-C(4)	1.343(4)	C(3)-C(4)-S(3)	122.8(2)
C(5)-C(6)	1.341(4)	S(4)-C(4)-S(3)	114.74(18)
C(5)-H(5)	0.9300	C(6)-C(5)-S(3)	118.9(3)
C(6)-C(7)	1.457(4)	C(6)-C(5)-H(5)	120.6
		S(3)-C(5)-H(5)	120.6
		C(5)-C(6)-C(7)	124.7(3)
		C(5)-C(6)-S(4)	117.3(2)
		C(7)-C(6)-S(4)	118.0(2)
		N(2)-C(7)-N(1)	125.4(3)
		N(2)-C(7)-C(6)	117.4(3)
		N(1)-C(7)-C(6)	117.2(3)
		N(4)-C(8)-N(3)	127.3(3)
		N(4)-C(8)-Cl(1)	116.9(3)
		N(3)-C(8)-Cl(1)	115.8(3)

Complex (**3**)ZnCl₂

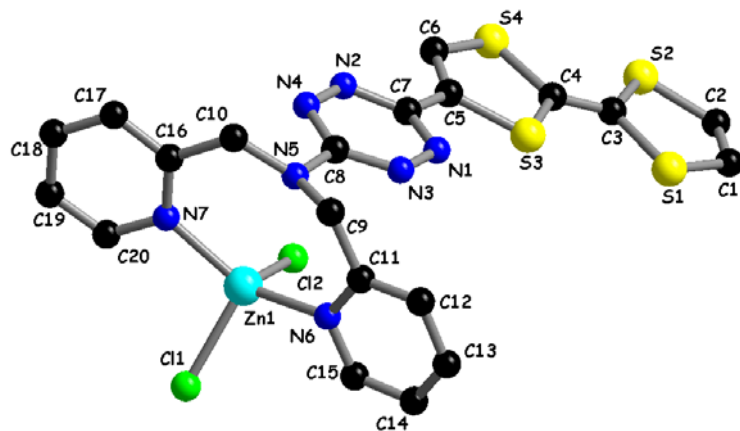


Fig. S4 Molecular structure of (**3**)ZnCl₂.

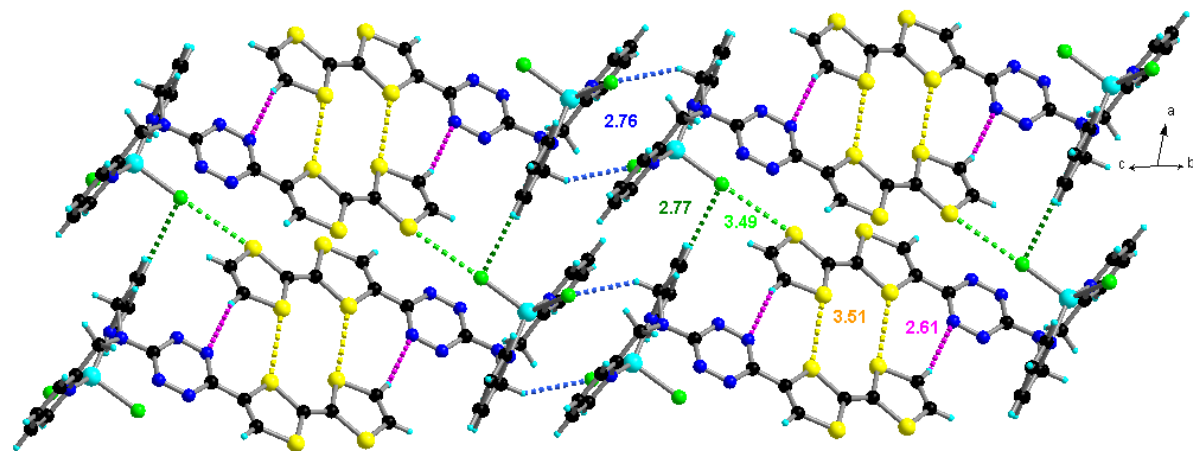


Fig. S5 Packing diagram for (**3**)ZnCl₂.

Table S3. Bond lengths (Å) and angles (°) for (**3**)ZnCl₂

Bond lengths (Å)		Bond angles (°)	
Zn(1)-N(7)	2.051(3)	N(7)-Zn(1)-N(6)	135.75(12)
Zn(1)-N(6)	2.056(3)	N(7)-Zn(1)-Cl(2)	106.30(9)
Zn(1)-Cl(2)	2.2643(12)	N(6)-Zn(1)-Cl(2)	99.97(8)
Zn(1)-Cl(1)	2.2862(11)	N(7)-Zn(1)-Cl(1)	102.48(8)
S(1)-C(1)	1.728(4)	N(6)-Zn(1)-Cl(1)	101.77(9)
S(1)-C(3)	1.762(3)	Cl(2)-Zn(1)-Cl(1)	108.94(5)
S(2)-C(2)	1.734(4)	C(1)-S(1)-C(3)	94.85(18)
S(2)-C(3)	1.763(4)	C(2)-S(2)-C(3)	94.43(19)
S(3)-C(5)	1.761(3)	C(5)-S(3)-C(4)	94.59(16)
S(3)-C(4)	1.762(4)	C(6)-S(4)-C(4)	94.34(17)
S(4)-C(6)	1.728(4)	N(3)-N(1)-C(7)	118.9(3)
S(4)-C(4)	1.769(3)	N(4)-N(2)-C(7)	117.2(3)
N(1)-N(3)	1.318(4)	N(1)-N(3)-C(8)	116.2(3)
N(1)-C(7)	1.339(4)	N(2)-N(4)-C(8)	117.4(3)
N(2)-N(4)	1.315(4)	C(8)-N(5)-C(10)	117.2(3)
N(2)-C(7)	1.357(4)	C(8)-N(5)-C(9)	116.8(3)
N(3)-C(8)	1.350(4)	C(10)-N(5)-C(9)	116.8(3)

N(4)-C(8)	1.354(5)	C(11)-N(6)-C(15)	118.2(3)
N(5)-C(8)	1.375(4)	C(11)-N(6)-Zn(1)	125.8(2)
N(5)-C(10)	1.470(4)	C(15)-N(6)-Zn(1)	115.4(2)
N(5)-C(9)	1.474(5)	C(16)-N(7)-C(20)	117.7(3)
N(6)-C(11)	1.327(4)	C(16)-N(7)-Zn(1)	127.3(2)
N(6)-C(15)	1.344(4)	C(20)-N(7)-Zn(1)	114.9(2)
N(7)-C(16)	1.332(4)	C(2)-C(1)-S(1)	118.3(3)
N(7)-C(20)	1.352(4)	C(2)-C(1)-H(1)	120.9
C(1)-C(2)	1.302(5)	S(1)-C(1)-H(1)	120.9
C(1)-H(1)	0.9300	C(1)-C(2)-S(2)	118.7(3)
C(2)-H(2)	0.9300	C(1)-C(2)-H(2)	120.7
C(3)-C(4)	1.333(4)	S(2)-C(2)-H(2)	120.7
C(5)-C(6)	1.331(5)	C(4)-C(3)-S(1)	121.5(3)
C(5)-C(7)	1.455(5)	C(4)-C(3)-S(2)	124.7(3)
C(6)-H(6)	0.9300	S(1)-C(3)-S(2)	113.76(17)
C(9)-C(11)	1.499(5)	C(3)-C(4)-S(3)	121.0(3)
C(9)-H(9A)	0.9700	C(3)-C(4)-S(4)	124.1(3)
C(9)-H(9B)	0.9700	S(3)-C(4)-S(4)	114.80(18)
C(10)-C(16)	1.504(5)	C(6)-C(5)-C(7)	128.5(3)
C(10)-H(10A)	0.9700	C(6)-C(5)-S(3)	116.7(3)
C(10)-H(10B)	0.9700	C(7)-C(5)-S(3)	114.7(3)
C(11)-C(12)	1.381(5)	C(5)-C(6)-S(4)	119.5(3)
C(12)-C(13)	1.379(6)	C(5)-C(6)-H(6)	120.3
C(12)-H(12)	0.9300	S(4)-C(6)-H(6)	120.3
C(13)-C(14)	1.361(6)	N(1)-C(7)-N(2)	124.5(3)
C(13)-H(13)	0.9300	N(1)-C(7)-C(5)	116.4(3)
C(14)-C(15)	1.363(5)	N(2)-C(7)-C(5)	119.1(3)
C(14)-H(14)	0.9300	N(3)-C(8)-N(4)	125.4(3)
C(15)-H(15)	0.9300	N(3)-C(8)-N(5)	116.4(3)
C(16)-C(17)	1.381(5)	N(4)-C(8)-N(5)	118.2(3)
C(17)-C(18)	1.374(6)	N(5)-C(9)-C(11)	114.2(3)
C(17)-H(17)	0.9300	N(5)-C(9)-H(9A)	108.7
C(18)-C(19)	1.363(6)	C(11)-C(9)-H(9A)	108.7
C(18)-H(18)	0.9300	N(5)-C(9)-H(9B)	108.7
C(19)-C(20)	1.372(5)	C(11)-C(9)-H(9B)	108.7
C(19)-H(19)	0.9300	H(9A)-C(9)-H(9B)	107.6
C(20)-H(20)	0.9300	N(5)-C(10)-C(16)	116.2(3)
		N(5)-C(10)-H(10A)	108.2
		C(16)-C(10)-H(10A)	108.2
		N(5)-C(10)-H(10B)	108.2
		C(16)-C(10)-H(10B)	108.2
		H(10A)-C(10)-H(10B)	107.4
		N(6)-C(11)-C(12)	121.2(3)
		N(6)-C(11)-C(9)	117.9(3)
		C(12)-C(11)-C(9)	120.8(3)
		C(13)-C(12)-C(11)	119.6(4)
		C(13)-C(12)-H(12)	120.2
		C(11)-C(12)-H(12)	120.2
		C(14)-C(13)-C(12)	118.9(4)
		C(14)-C(13)-H(13)	120.5
		C(12)-C(13)-H(13)	120.5
		C(13)-C(14)-C(15)	118.5(4)
		C(13)-C(14)-H(14)	120.7
		C(15)-C(14)-H(14)	120.7
		N(6)-C(15)-C(14)	123.3(4)
		N(6)-C(15)-H(15)	118.3
		C(14)-C(15)-H(15)	118.3
		N(7)-C(16)-C(17)	121.4(3)
		N(7)-C(16)-C(10)	119.9(3)
		C(17)-C(16)-C(10)	118.6(3)

C(18)-C(17)-C(16)	119.8(4)
C(18)-C(17)-H(17)	120.1
C(16)-C(17)-H(17)	120.1
C(19)-C(18)-C(17)	119.4(4)
C(19)-C(18)-H(18)	120.3
C(17)-C(18)-H(18)	120.3
C(18)-C(19)-C(20)	118.0(4)
C(18)-C(19)-H(19)	121.0
C(20)-C(19)-H(19)	121.0
N(7)-C(20)-C(19)	123.6(4)
N(7)-C(20)-H(20)	118.2
C(19)-C(20)-H(20)	118.2

Electrochemical studies. Cyclic voltammetry measurements were carried out with a Biologic SP-150 potentiostat in a glove box containing dry, oxygen-free (<1 ppm) argon at 293 K, by using a three-electrode cell equipped with a platinum millielectrode of 0.126 cm² area, an Ag/Ag⁺ pseudo-reference electrode and a platinum wire counter electrode. The potential values were then re-adjusted with respect to the saturated calomel electrode (SCE). The electrolytic media involved a 0.1 mol/L solution of (*n*-Bu₄N)PF₆ in dichloromethane/acetonitrile 1/1. All experiments were performed at room temperature at 0.1 V/s.

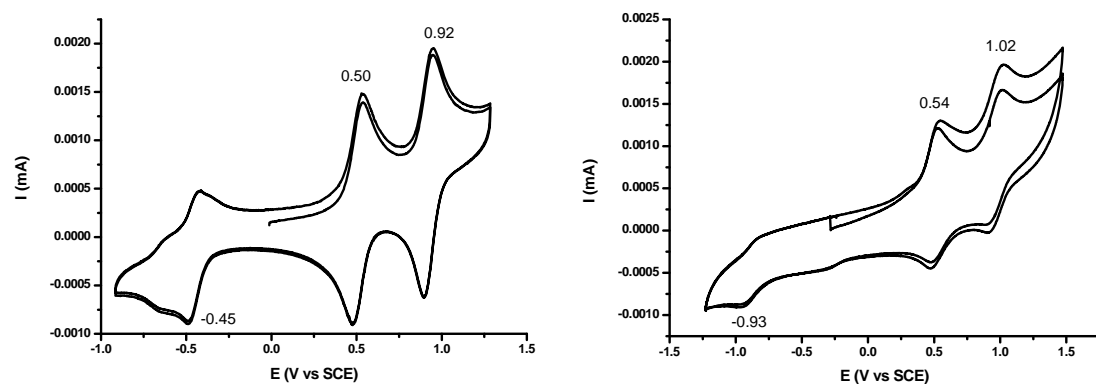


Fig. S6 Cyclic voltammetry performed in CH₂Cl₂/MeCN (1:1) in the presence of (*n*-Bu₄N)PF₆ (0.1 M) at a scan rate of 0.1 V·s⁻¹ for **1** (left) and **3** (right).

UV-Vis spectroscopy and photophysics

UV-Vis spectra for TTF, 3,6-dichloro-1,2,4,5-tetrazine (3,6-Cl₂-TTZ) and **3** were recorded in DCM solutions using a Lambda 19 PERKIN ELMER Spectrometer.

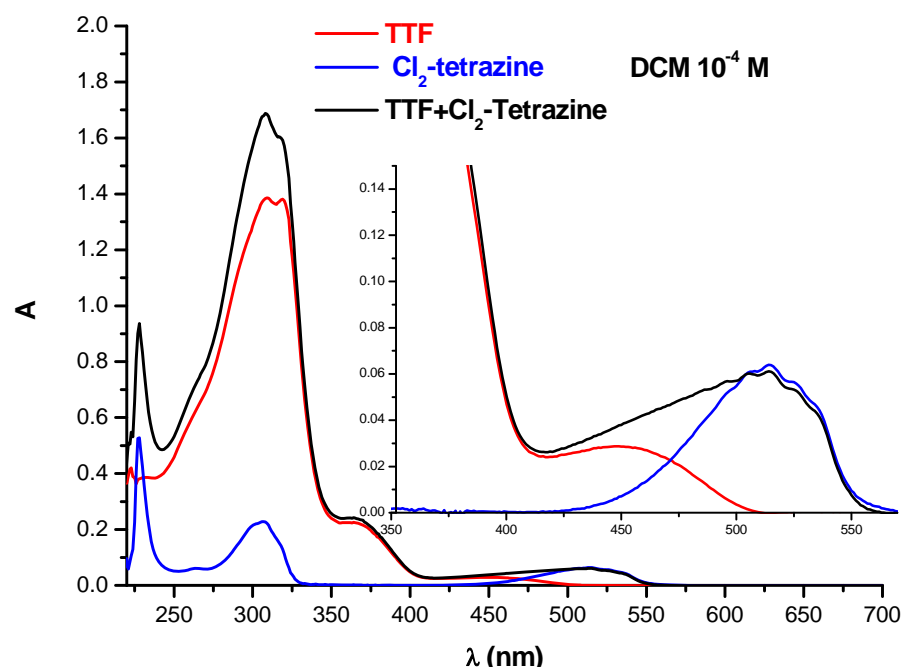


Fig. S7 UV-Vis spectra of TTF, dichloro-tetrazine and the mixture of the two, in DCM (10^{-4} M) with a detailed area inset.

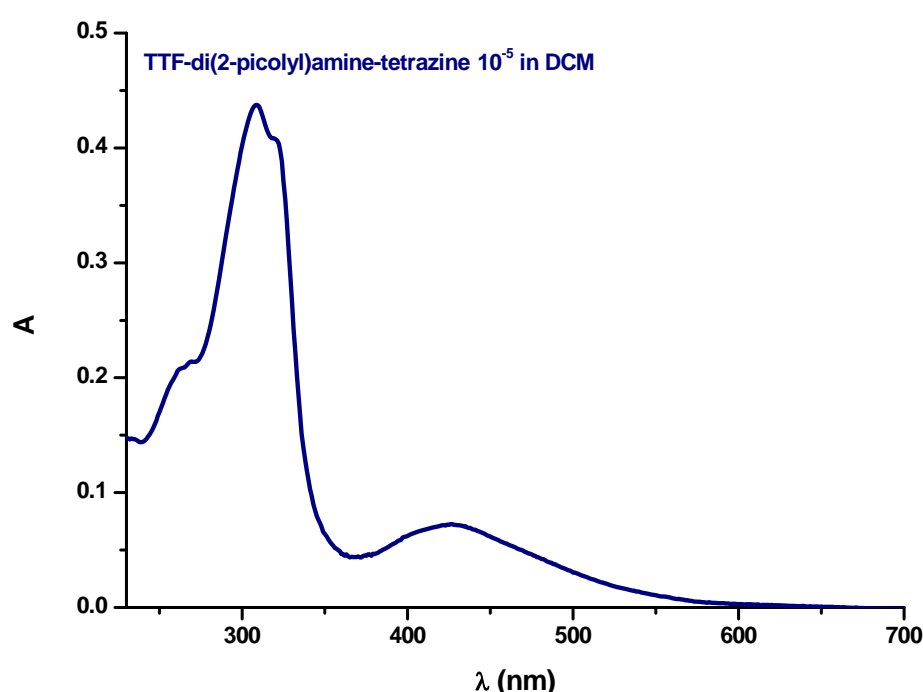


Fig. S8 UV-Vis spectrum of TTF-di(2-picoly)amine-1,2,4,5-tetrazine (**3**), 10^{-5} M solution in DCM; $\lambda_{\text{max}} = 427$ nm (23420 cm^{-1}); $\epsilon = 7000 \text{ L} \cdot \text{mol}^{-1} \cdot \text{cm}^{-1}$.

Solvents always of the best available quality for photophysics and spectroelectrochemistry were purchased from commercial sources and used as received without further purification.

UV-Vis absorption spectra were measured on a Cary 5000 spectrophotometer. Steady-state emission spectra were recorded on a Fluorolog 3 spectrophotometer. In most cases, the preparation of samples in different solvents was started from an initial concentrated DCM standard solution. The volume fraction of DCM in the final solution was less than 5 % in all of the tested solution samples. Solution samples with proper concentrations were prepared by optical dilution for steady-state photoluminescence ($OD < 0.1$) and deoxygenated for 30 min in a 1 cm path-length quartz cell prior to measurements. Precautions were taken to limit exposure of the photosensitive complexes to light in between measurements and during bubbling.

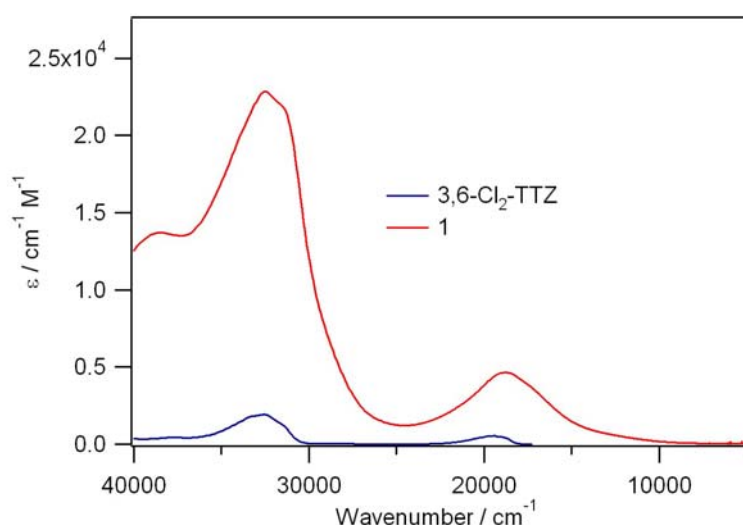


Fig. S9 UV-vis absorption spectra of **1** and 3,6-Cl₂-TTZ in DCM at room temperature.

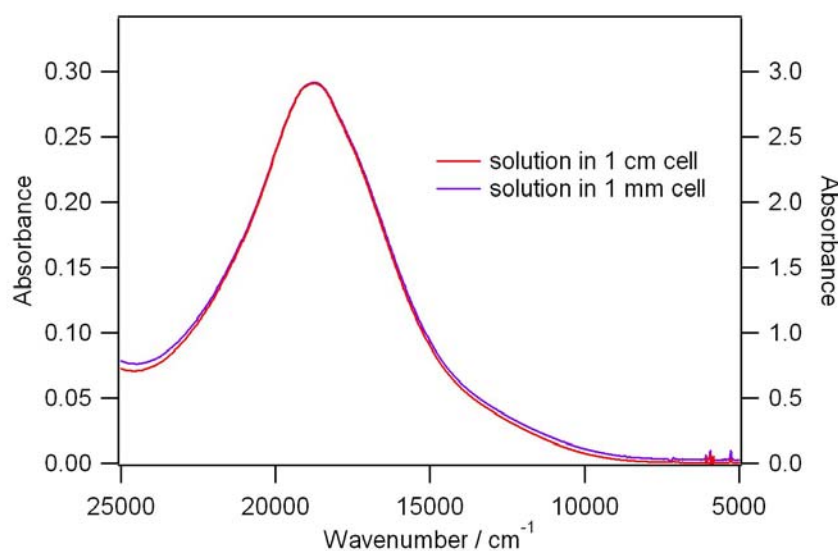


Fig. S10 UV-vis absorption spectra of **1** in DCM solution in different cells and concentrations at room temperature. Only the ICT is shown.

Table S4. Photophysics for **1** in DCM at room temperature.

Entry	$\nu_{\text{abs}} / \text{cm}^{-1}$ ($\epsilon / \text{L} \cdot \text{mol}^{-1} \cdot \text{cm}^{-1}$)	$\nu_{\text{em}} / \text{cm}^{-1}$
1	32468 (22100), 31447 (21100), 18797 (4200)	non-emissive

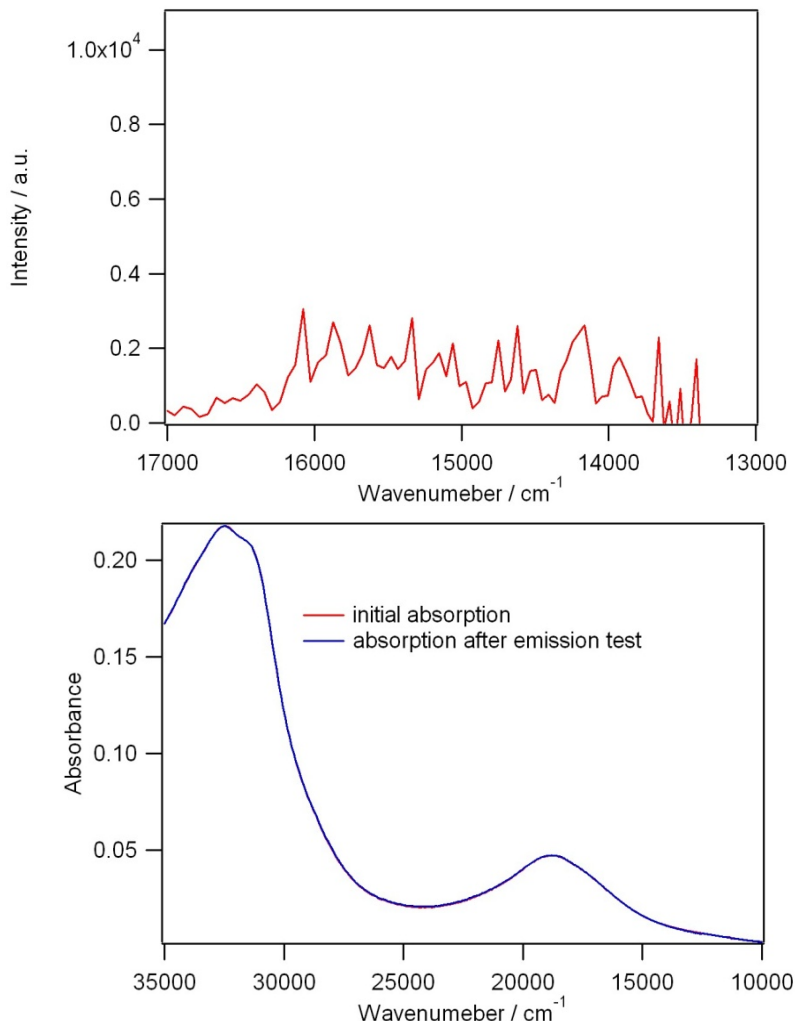


Fig. S11 Emission spectrum of **1** (1×10^{-5} M) in DCM at room temperature. ($\lambda_{\text{ex}} = 530$ nm, 18870 cm⁻¹, top) and absorption spectra of **1** (1×10^{-5} M, bottom) before and after emission-excitation measurements.

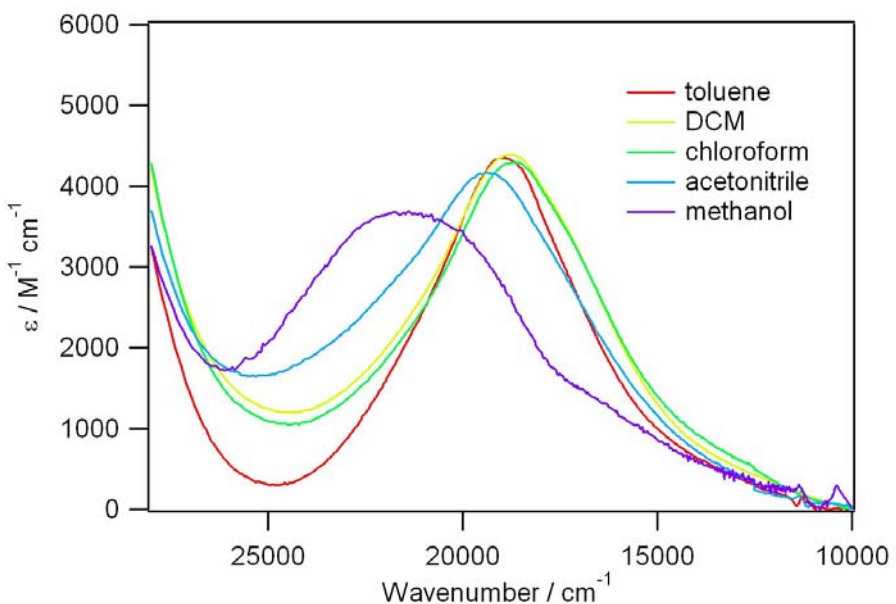


Fig. S12 ^1ICT absorption band of **1** in (a) toluene, (b) DCM, (c) chloroform, (d) acetonitrile and (e) methanol.

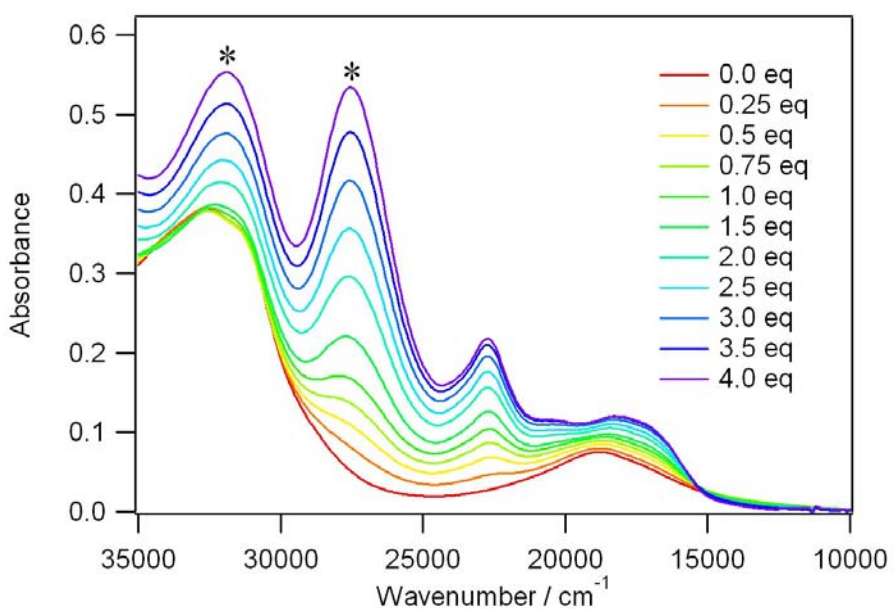


Fig. S13 UV-vis absorption of **1** ($1.8 \times 10^{-5} \text{ M}$) during chemical oxidation by successive addition of oxidant FeCl_3 in DCM at room temperature. * unreacted FeCl_3 .

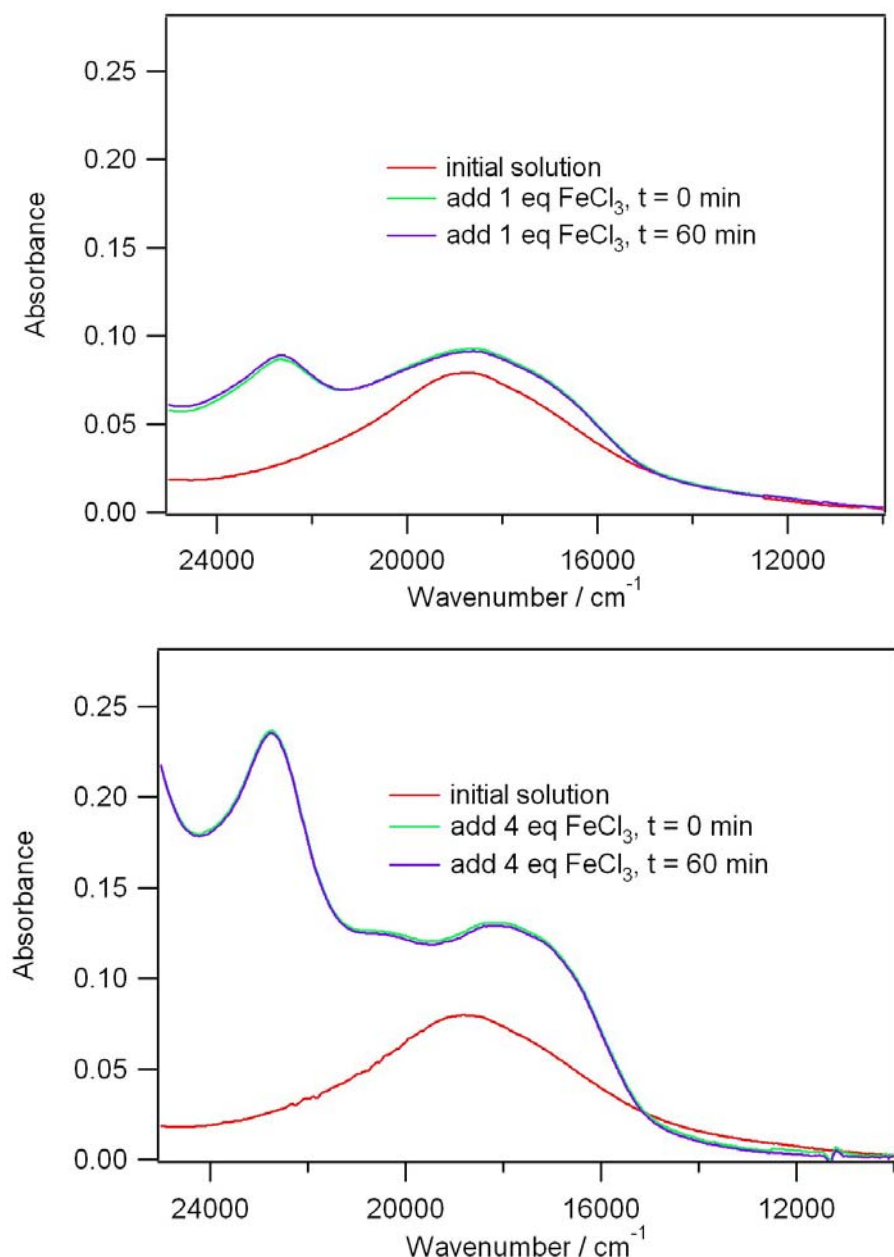


Fig. S14 UV-vis absorption of **1** (1.9×10^{-5} M) during chemical oxidation by oxidant FeCl_3 in DCM at room temperature. * unreacted FeCl_3 .

Theoretical calculations on 1

Density functional theory (DFT) [1,2] has been applied to the determination of the ground-state geometry of the isolated molecule, and its lowest-lying singlet excited states have been characterized within time-dependent DFT (TDDFT) [3-5]. All calculations have been performed with the Gaussian 09 program package [6]. The geometry optimization was carried out with the PBE functional [7,8] and the TDDFT electronic excitation calculations with the PBE1PBE (aka PBE0) functional [9,10]. The atoms were described by Dunning's correlation consistent basis sets augmented with diffuse functions [11,12]: namely, the aug-cc-pVDZ basis set for the H atoms, and the aug-cc-pVTZ basis set for the C, N, S, and Cl atoms. The ground-state geometry of the molecule is C_1 resulting from the pseudo-Jahn-Teller instability of the geometry of C_s symmetry as shown in Fig. S15.

References :

- [1] P. Hohenberg, W. Kohn, *Phys. Rev.* **1964**, *136*, B864-B871.
- [2] W. Kohn, L. J. Sham, *Phys. Rev.* **1965**, *140*, A1133-A1138.
- [3] M. E. Casida, Time-Dependent Density Functional Response Theory for Molecules. In *Recent Advances in Density Functional Methods*; Chong, D. P., Ed.; World Scientific: Singapore, 1995; Vol. 1.
- [4] R. Bauernschmitt, R. Ahlrichs, *Chem. Phys. Lett.*, **1996**, *256*, 454-464.
- [5] R. E. Stratmann, G. E. Scuseria, M. J. Frisch, *J. Chem. Phys.*, **1998**, *109*, 8218-8224.
- [6] Gaussian 09, Revision C.01, M. J. Frisch, G. W. Trucks, H. B. Schlegel, G. E. Scuseria, M. A. Robb, J. R. Cheeseman, G. Scalmani, V. Barone, B. Mennucci, G. A. Petersson, H. Nakatsuji, M. Caricato, X. Li, H. P. Hratchian, A. F. Izmaylov, J. Bloino, G. Zheng, J. L. Sonnenberg, M. Hada, M. Ehara, K. Toyota, R. Fukuda, J. Hasegawa, M. Ishida, T. Nakajima, Y. Honda, O. Kitao, H. Nakai, T. Vreven, J. A. Montgomery, Jr., J. E. Peralta, F. Ogliaro, M. Bearpark, J. J. Heyd, E. Brothers, K. N. Kudin, V. N. Staroverov, T. Keith, R. Kobayashi, J. Normand, K. Raghavachari, A. Rendell, J. C. Burant, S. S. Iyengar, J. Tomasi, M. Cossi, N. Rega, J. M. Millam, M. Klene, J. E. Knox, J. B. Cross, V. Bakken, C. Adamo, J. Jaramillo, R. Gomperts, R. E. Stratmann, O. Yazyev, A. J. Austin, R. Cammi, C. Pomelli, J. W. Ochterski, R. L. Martin, K. Morokuma, V. G. Zakrzewski, G. A. Voth, P. Salvador, J. J. Dannenberg, S. Dapprich, A. D. Daniels, O. Farkas, J. B. Foresman, J. V. Ortiz, J. Cioslowski, and D. J. Fox, Gaussian, Inc., Wallingford CT, 2010.
- [7] J. P. Perdew, K. Burke, M. Ernzerhof, *Phys. Rev. Lett.*, **1996**, *77*, 3865-3868.
- [8] J. P. Perdew, K. Burke, M. Ernzerhof, *Phys. Rev. Lett.*, **1997**, *78*, 1396.
- [9] K. Burke, M. Ernzerhof, J. P. Perdew, *Chem. Phys. Lett.*, **1997**, *265*, 115-120.
- [10] C. Adamo, V. Barone, *J. Chem. Phys.*, **1999**, *110*, 6158-6169.
- [11] T. H. Dunning, Jr. *J. Chem. Phys.*, **1989**, *90*, 1007-1023.
- [12] D. E. Woon, T. H. Dunning, Jr. *J. Chem. Phys.* 1993, **98**, 1358-1471.

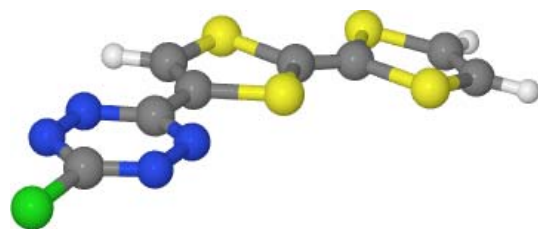


Fig. S15 Optimized geometry of C₁ symmetry of the compound **1**.

Table S5: Characterization of the 14 lowest-lying singlet excited state of the compound **1**.

State	Energy (cm ⁻¹)	Oscillator strength	Major MO → MO contributions (%)
S ₁	10388	0.019	HOMO → LUMO (100)
S ₂	15878	0.106	HOMO → LUMO+1 (100)
S ₃	18795	0.004	HOMO-2 → LUMO+1 (100)
S ₄	21698	0.000	HOMO → LUMO+2 (100)
S ₅	25166	0.004	HOMO-1 → LUMO (100)
S ₆	25198	0.000	HOMO-2 → LUMO+1 (100)
S ₇	29020	0.012	HOMO → LUMO+3 (98)
S ₈	31715	0.103	HOMO-1 → LUMO+1 (39) HOMO → LUMO+7 (38) HOMO → LUMO+8 (10)
S ₉	31939	0.192	HOMO -1 → LUMO+1 (64) HOMO → LUMO+7 (20)
S ₁₀	32938	0.054	HOMO → LUMO+4 (19) HOMO → LUMO+5 (19) HOMO → LUMO+8 (16) HOMO → LUMO+9 (15) HOMO → LUMO+10 (10)
S ₁₁	33266	0.057	HOMO-3 → LUMO (77)
S ₁₂	34316	0.116	HOMO → LUMO+4 (32) HOMO → LUMO+5 (29) HOMO → LUMO+6 (29)
S ₁₃	34418	0.067	HOMO → LUMO+4 (35) HOMO → LUMO+6 (29)
S ₁₄	34816	0.161	HOMO → LUMO+6 (34) HOMO → LUMO+5 (31) HOMO → LUMO+8 (16)

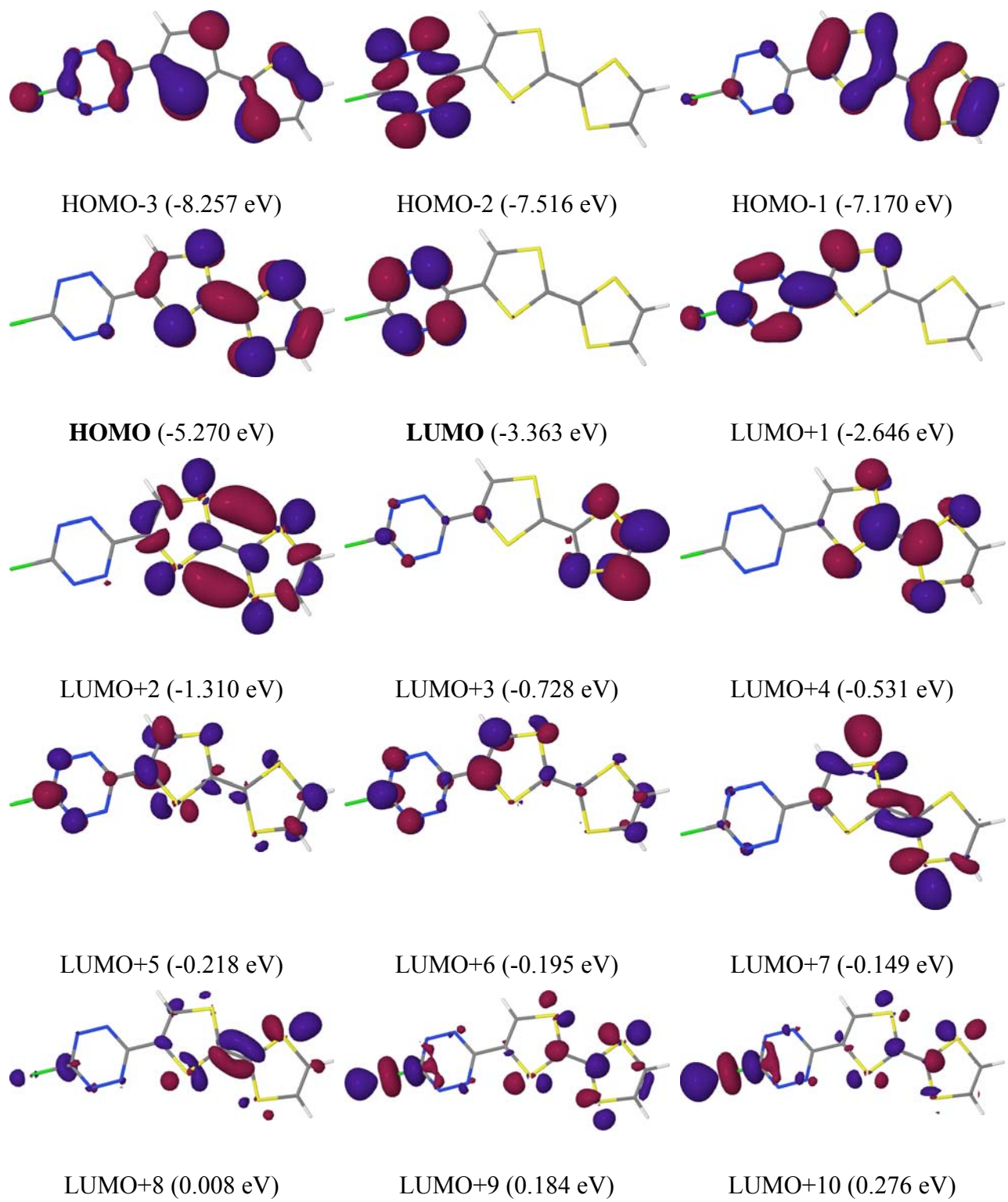


Fig. S16 Molecular orbitals of compound 1.

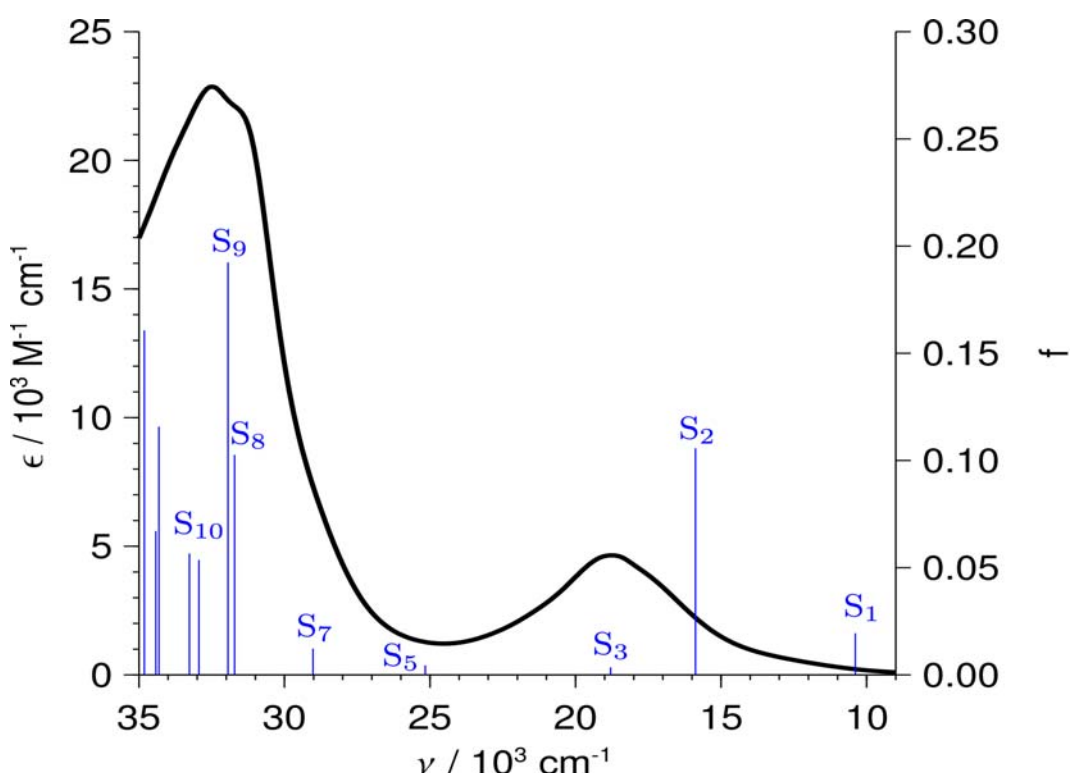


Fig. S17 Electronic absorption spectra of **1** in DCM with the calculated $S_0 \rightarrow S_n$ transitions.